VNU Journal of Science: Natural Sciences and Technology

Journal homepage: https://js.vnu.edu.vn/NST

Original Article

A Gold Nanoparticle-based SERS Platform for Trace-Level Detection of Organic Contaminants in Municipal Tap Water

Nguyen Kien Cuong*

VNU University of Engineering and Technology, 144 Xuan Thuy, Cau Giay, Hanoi, Vietnam

Received 03rd October 2025
Revised 18th December 2025; Accepted December 2025

Abstract: Highly sensitive detection techniques are required because harmful organic residues in drinking water, such as dyes, antibiotics, and oils, pose significant health risks. We investigate surface-enhanced Raman scattering (SERS), which achieves sensitivity down to 10^{-4} M, because Conventional Raman spectroscopy cannot reliably detect dye concentrations below 10^{-9} M. Using sodium citrate as a reducing agent, we synthesized 10-20 nm gold nanoparticles from $HauCl_4 \cdot 3H_2O$ and deposited them onto glass to create a 30-54 nm rough layer to create a SERS substrate. Raman signals are significantly amplified by this nanoscale roughness due to increased local electromagnetic fields. To evaluate the sensing performance of the substrate, Rhodamine 6G (Rh6G) solutions with concentrations from 10^{-4} M to 10^{-9} M were analyzed using a Raman spectrometer. Distinct spectral peaks of Rh6G were clearly observed even at 10^{-9} M, whereas standard Raman spectroscopy on smooth glass failed to detect signals at comparable concentrations. This exceptional sensitivity results from strong localized surface plasmon resonance (LSPR) at hotspots in the ~30 nm thick gold nanoparticle film, where Rh6G signals were amplified several-fold. The substrate's substantial signal enhancement demonstrates its potential for detecting trace dye residues in drinking water using portable Raman spectrometers for convenient field deployment.

Keywords: Surface-enhanced Raman Scattering (SERS), gold nanoparticles (AuNPs), Rhodamine 6G (Rh6G) dye, hotspots, localized surface plasmon resonance (LSPR).

* Corresponding author.
E-mail address: cuongnk@vnu.edu.vn

https://doi.org/10.25073/2588-1140/vnunst.5944

1. Introduction

Organic pollutants in municipal drinking water sources are detrimental to human health. Pesticides, pharmaceuticals, industrial compounds, antibiotics, herbicides, and polycyclic aromatic hydrocarbons (PAHs) are trace-level contaminants. Even though these pollutants usually don't reach levels that are higher than regulatory limits, their complicated and long-lasting molecular structures make people very worried about the possible health effects of long-term exposure to them [1-3]. Liquid chromatography-tandem mass spectrometry (LC-MS/MS) and gas chromatography-tandem mass spectrometry (GC-MS/MS) are two common analytical methods that are highly sensitive and selective for detecting these types of contaminants.

However, their practical implementation encounters considerable limitations owing to the need for advanced laboratory infrastructure, labor-intensive sample preparation procedures, and high operational costs [4-6]. These limitations render them unsuitable for regular and real-time monitoring, creating a need for new methods that allow for rapid field measurements of contaminant species while delivering strong analytical results.

Surface-enhanced Raman spectroscopy (SERS) is a highly sensitive analytical method for identifying trace-levels of organic contaminants in municipal water systems. SERS provides a rapid, non-destructive, and label-free alternative for detecting organic molecules at incredibly low concentrations [7]. For certain compounds, the synergistic mechanisms underpinning this method can achieve detection sensitivities as high as parts-per-billion (ppb) or even parts-per-trillion (ppt) [8-10]. The immobilization of thiol-functionalized gold nanoparticles (AuNPs) onto mesoporous silica (MPS-SH) substrates is a recent development in substrate design. These developments have facilitated the creation of localized surface plasmon resonance (LSPR) hotspots through substrate structure optimization, amplifying the SERS effect for ultrasensitive analyte detection. For example, it has been reported that Rhodamine 6G has a detection limit of 2.6×10^{18} particles/mL of AuNP at concentrations below 10^{-6} M [11].

Current research focuses on creating SERS substrates that can detect analytes at much lower concentrations using portable, handheld Raman spectrometers. Compared to the previous detection limits of 10^{-6} M for Rh6G using 67 nm AuNPs immobilized on honeycomb-like polymeric films, the reported limit of detection for PAHs using AuNP-based substrates was 1.2×10^{-8} M [12]. Combining a handheld SERS-enabled device with liquid-liquid or solid-phase microextraction techniques may increase the applications for the quick field analysis of 8 nM thiram (TMTD) and 8 nM malachite green (MG) related to surface organic residues (SORs) [13].

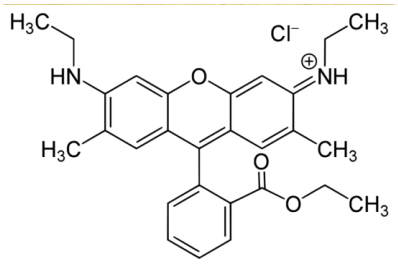

Figure 1. Typical molecular formula of a Rh6G indicator.

Surface-enhanced Raman spectroscopy (SERS) based AuNPs is a promising method for tracking organic pollutants in municipal water systems. This study focuses on the laboratory synthesis of 10-20 nm AuNPs to create a SERS-based platform. For the dye rhodamine 6G (Rh6G) deposited on SERS substrates, the experimental results successfully showed enhanced Raman signals, allowing for sensitive detection at concentrations as low as 10^{-9} M. By integrating it with a portable Raman spectrometer, its application was extended beyond monitoring municipal water to include food products, biological materials, and pharmaceuticals. Crucially, this approach

complies with the safety regulations set by the Ministry of Health, confirming its potential to improve public health.

2. Experimental

2.1. Synthesis of Gold Nanoparticles

The chemical agents used in this study included 3-Aminopropyl triethoxysilane (APTES) $C_2H_5O)_3$-Si-C_3H_6-NH_2, tetrachloroauric acid trihydrate at 99.5% purity ($HAuCl_4 \bullet 3H_2O$), and tetrakis(hydroxymethyl) phosphonium chloride $[(CH_2OH)_4P]Cl$, all procured from Merck and Sigma-Aldrich Co. Ltd. In addition to these precursors, a selection of solvents was employed, specifically formaldehyde (HCHO) at a concentration of 37-38%, trisodium citrate ($Na_3C_6H_5O_7$), ethanol (C_2H_5OH) at approximately 99.9% purity, potassium carbonate (K_2CO_3), sodium hydroxide (NaOH), potassium hydroxide (KOH), and deionized water. These materials are necessary for the synthesis of AuNPs, the fundamental components of SERS substrates. Using the Turkevich method [14], which uses trisodium citrate as the reducing agent and $HAuCl_4$ as the gold precursor, we created gold nanoparticles. The synthesis was completed when the suspension solution's color stabilized, signifying successful AuNP formation. We kept the AuNP suspension at 4 ℃ after allowing it to naturally cool to room temperature following synthesis. The following is the process used to create Au nanoparticles.

2.2. Synthesis of Gold Nanoparticles in Solution

The procedure for synthesizing AuNPs was as follows:

* Preparation of gold hydroxide solvent:

$K_2CO_3 + H_2O \rightarrow HCO_3^- + 2K^+ + OH^-$

$HAuCl_4 + (4\text{-}x)\ OH^- \rightarrow [AuCl_x\ (OH)_{4-x}]$-; x = 0-4.

$[P(CH_2OH)_4]\ Cl + NaOH \rightarrow P(CH_2OH)_3 + H_2O + HCHO + NaCl$.

* Synthesis of AuNPs:

$HAuCl_4 + 2HCHO + 2H_2O \rightarrow Au^0 + 2HCOOH + 4HCl + ½\ H_2$

Spherical gold nanoparticles were synthesized to prepare a colloidal solution. When this solution was drop-cast onto a solid substrate, such as a glass slide, sub-monolayers of AuNPs were deposited on the substrate. The nanoparticles were randomly distributed across the surface, and their density depended on the concentration of the colloidal solution and the adsorption properties of the substrates.

2.3. Surface Functionalization of Glass Substrates by Primary Amine (-NH_2) Groups

Glass substrates measuring 1 cm × 2.54 cm were subjected to an extensive cleaning process involving immersion in a 10 mL solution of 1 M KOH, followed by sonication for two cycles of five minutes each. This procedure effectively removed the surface contaminants from the samples. Subsequently, the substrates were immersed in ethanol overnight to facilitate the formation of hydroxyl (–OH) groups, which are essential for subsequent surface functionalization.

As gold nanoparticles carry a negative surface charge, effective immobilization on the substrate requires the introduction of a positive surface charge. To achieve this requirement, glass substrates were treated with a solution of APTES (3-aminopropyltriethoxysilane). Through hydrolysis and condensation reactions with surface hydroxyl groups, primary amine (-NH_2) functionalities were incorporated, rendering the surface suitable for the AuNP attachment.

= Si-OH + $(C_2H_5$-O)-Si-$(CH_2)_3$-$NH_2 \rightarrow$ Si-O-Si-$(CH_2)_3$-NH_2

2.4. Deposition of AuNPs on a Surface-modified Glass Substrate

The synthesized AuNPs were immobilized onto glass substrates that had been modified with amine groups (-NH_2). This was achieved through strong electrostatic interactions between the negatively charged AuNPs and positively charged -NH_2 groups. This binding mechanism, primarily driven by electrostatic

attraction, ensures stable adhesion and reduces the risk of nanoparticle detachment from the target cell surface. The initially deposited AuNPs served as a nucleation layer that facilitated the vertical stacking of additional nanoparticles on the substrate. Importantly, the size of these initial AuNP nuclei significantly influenced the surface roughness of the resulting multilayered structure, as described in references [9-11].

To thoroughly analyze the topographical and optical characteristics of the stacked AuNP layers, we employed scanning electron microscopy (SEM), atomic force microscopy (AFM), and UV-visible spectroscopy. Additionally, the AuNP-deposited surface was carefully engineered to enhance the Raman signal intensity in conjunction with the fluorescent probe, Rh6G.

2.4. Determination of Enhancing Raman's Spectrum of Rh6G Analyte on a SERS Substrate

Rhodamine 6G (Rh6G, $C_{28}H_{31}N_2O_3Cl$) is a fluorescent dye that is employed as a probe to assess the enhancement of Raman signals of Rh6G analyte on SERS-based AuNP substrates. For this analysis, Rh6G powder was dissolved in solutions with concentrations ranging from 10^{-4} M to 10^{-9} M. A droplet of each analyte solution was drop-cast onto the SERS-based substrate, and the Rh6G analyte was illuminated with a 532 nm laser. The Raman scattering generated from the SERS surface was collected and analyzed using a Raman spectrometer (Labram HR Evolution, HORIBA). The observed enhancement of the Raman signal from Rh6G on the AuNP layer provided a quantitative assessment of the plasmonic resonance effect.

3. Results and Discussion

3.1. Absorption Spectrum of Gold Nanoparticles

The UV-Vis absorption spectrum obtained from the aqueous dispersion of the synthesized nanoparticles exhibits a prominent, single peak centered at 510 nm (fig.2). This band is the characteristic optical signature of the Localized Surface Plasmon Resonance (LSPR) phenomenon in spherical Gold Nanoparticles (AuNPs), thereby confirming the successful synthesis and the Au composition of the 10-20 nm particles [15]. The narrowness of the peak suggests a uniform particle size distribution. Crucially, the 510 nm LSPR maximum is ideally positioned in close spectral proximity to the 532 nm excitation laser utilized for SERS measurements, ensuring efficient electromagnetic coupling. This high degree of plasmonic activity is the fundamental optical prerequisite that, when combined with the surface roughness and particle aggregation leading to "hotspots" , enables the remarkable Surface-Enhanced Raman Scattering (SERS) enhancement necessary for the ultra-trace detection of Rh6G at concentrations as low as 10^{-9} M.

3.2. The Typical Topography of SEM Images for a SERS-based AuNP Layer

While we found that the nanoparticles were spread fairly evenly across the surface, we also noticed something interesting: tiny nanoscale cracks between some of the clustered particles. These small gaps are actually quite valuable because they create what scientists call plasmonic "hot spots", think of them as concentrated pockets where the surface plasmon resonance (LSPR) effects become much more intense. These hot spots are what give the material its remarkable ability to boost surface-enhanced Raman scattering (SERS) signals. Our SEM analysis backed this up, showing that the gold nanoparticles were indeed well distributed across the substrate.

To understand why these hotspots form in the first place, we need to look at what happens during the synthesis process itself. The formation of these LSPR-active hotspots is directly tied to how the gold nanoparticles naturally tend to aggregate. As we synthesize the material, gold atoms attach themselves to existing nuclei, the tiny seeds that start the

growth process. Even small differences in where these initial nuclei are positioned can cause the gold atoms to cluster together in certain spots. This natural tendency resulted in the formation of nanostructured regions with surfaces that are not perfectly smooth but rather have an uneven, textured quality.

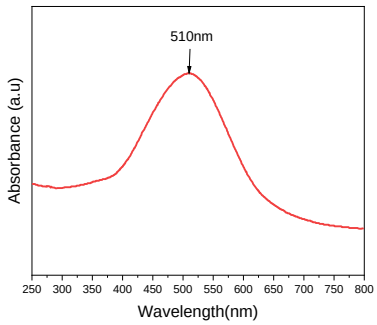

Figure 2. Typical UV-vis absorption spectrum of synthesized AuNPs at around of 20 nm diameter.

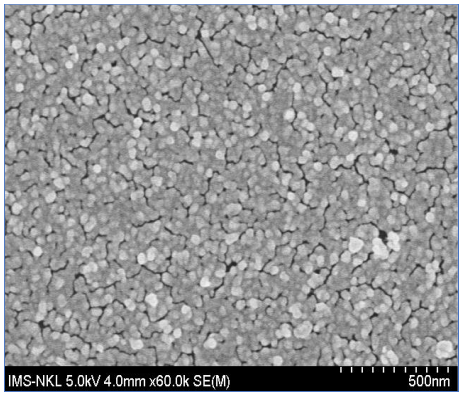

Figure 3. SEM image of SERS-based AuNPs (10-20 nm) forming a sparse submonolayer on a glass substrate via drop-casting.

When we took a closer look at the surface structure using atomic force microscopy, the details became even clearer. The AFM image (Figure 4) showed us that the gold nanoparticle layer averaged about 30 nm in thickness. By analyzing the surface roughness, we determined that these plasmonically active regions were typically made up of 2 to 3 aggregated particles stacked together, with each individual particle measuring somewhere between 10 and 20 nm. The three-dimensional roughness profile we obtained from AFM matched up nicely with what we saw in the cross-sectional SEM measurements (Figure 5), confirming that the gold nanoparticle layer thickness wasn't uniform, it ranged anywhere from 30 to 54 nm depending on where you looked across the substrate surface. These differences in both thickness and surface roughness aren't just incidental details; they play a crucial role in determining how strong the Raman signals will be. Now, here is where everything comes together in a practical demonstration of the material's capabilities. When we excited a 532 nm laser onto the gold nanoparticle film, something remarkable happened. The film's layered architecture, combined with those hotspots formed by the nanoparticle clusters, worked together to amplify the plasmonic coupling effect. This amplification translated directly into significantly stronger SERS signals from our test molecule, Rhodamine 6G.

Figure 3 and 4 show that more hotspots are linked to higher LSPR signals in the SEM and AFM images, respectively. The SEM (surface cracks) and AFM (surface roughness) analyses suggest that the surface roughness, film thickness, and arrangement of the particles all affect the plasmonic behavior.

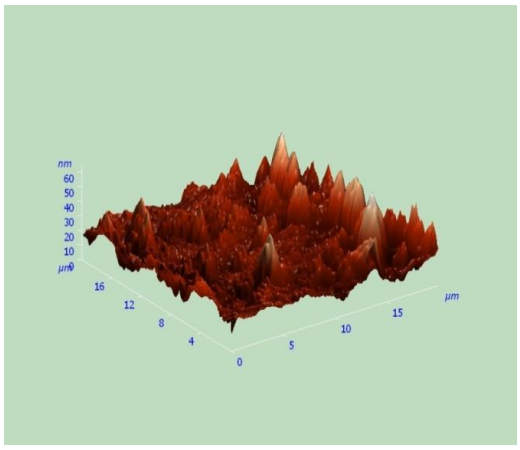

Figure 4. An AFM image showing the roughness of the SERS-based AuNP layer.

The SEM image in Figure 3 (at 500× magnification) shows that the gold nanoparticles are mostly spread evenly across the glass, with some small gaps between groups of particles. These gaps likely create plasmonic hotspots, which increase the surface plasmon resonance and improve the SERS performance.

The combination of AFM and SEM data confirmed that the surface roughness, layer thickness, and aggregation patterns collectively influenced the plasmonic behavior of the material. Furthermore, cross-sectional SEM imaging provides additional validation of these findings, demonstrating how structural features such as particle clustering and layer uniformity modulate SERS performance. Overall, the SEM results show that the AuNPs were mostly well-dispersed.

3.3. Raman Amplitude's Enhancement of Rh6G Deposited on AuNP-layer

The SERS-active gold nanoparticle (AuNP) layer exhibited characteristic absorption peaks linked to localized surface plasmon resonance (LSPR) in the range of approximately 520 - 530 nm. As the thickness of the AuNP layers increased, these peaks experienced a red shift, which was attributed to the gradual enlargement of the nanoparticles during synthesis. Although specific measurements are not detailed here, this red shift implies uneven particle growth, likely owing to varying levels of interparticle interactions.

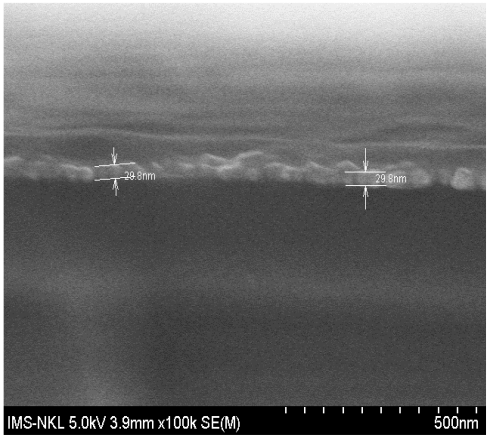

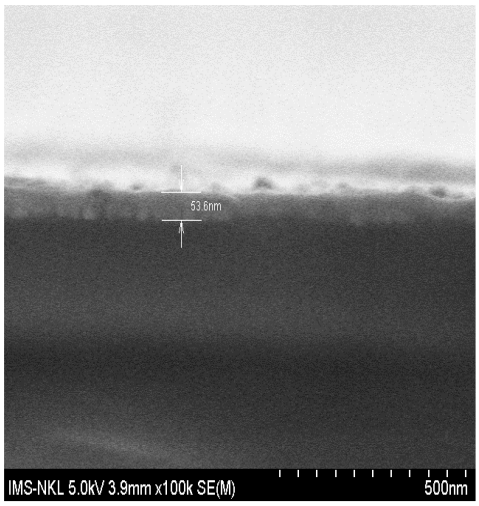

Figure 5. SEM images of the SERS-based AuNP layer, showing cross-sectional thickness on a glass substrate prepared via drop-casting.

The diversity in these interactions seems to lead to different growth rates among the AuNPs, resulting in variations in the optical absorption spectra and indicating that the particle size increase was inconsistent across the substrate. Subsequently, the Raman signal intensities of Rhodamine 6G (Rh6G) solutions at various concentrations were measured using a LabRAM HR Evolution spectrometer (Horiba Co. Ltd.), employing a 532 nm excitation laser. The enhancement of Raman signals was evaluated on both a bare glass substrate and the SERS based on AuNP layer, which exhibited notably significant signal amplification, confirming its role in enhancing the Raman response of the Rh6G analyte.

Initial measurements of Rh6G powder at high concentration on the glass substrate revealed distinct Raman peaks located at 613 cm^{-1} (*C–C–C ring in-plane bending*), 774 cm^{-1} (*C–H out-of-plane bending*), 1189 cm^{-1} (*C–C stretching*), 1308 cm^{-1} (*CH_2 twisting*) 1360 cm^{-1}, (*aromatic C–C stretching*), 1509 cm^{-1} (*C–C stretching*), 1572 cm^{-1}, 1647 cm^{-1} (*C–C stretching*) corresponding to Rh6G dye substance, respectively (See Fig. 6).

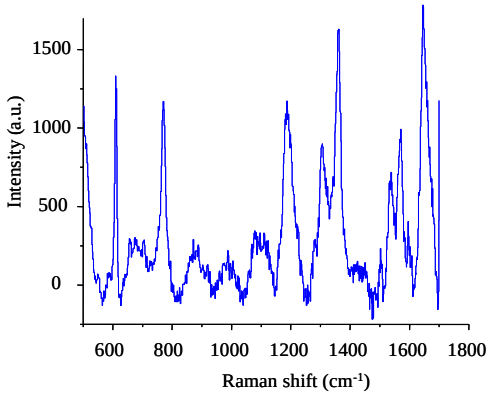

Figure 6. Typical Raman peaks of Rh6G powder on a blank glass surface.

When a Rhodamine 6G (Rh6G) solution diluted to a concentration of 10^{-4}M was applied to a plain glass substrate, no distinct Raman peaks of Rh6G were detected. This absence of a signal is likely due to the concentration being below the detection threshold of conventional Raman spectroscopy, highlighting the limitations of this method at such low analyte concentrations. Conversely, the same Rh6G concentration produced clearly discernible Raman peaks when examined using an SERS-based AuNP substrate under the same experimental conditions.

As illustrated in Figure 7, the Raman spectrum of Rh6G on the AuNP substrate exhibited distinct peaks at 613 cm^{-1}, 774 cm^{-1}, 1189 cm^{-1}, 1308 cm^{-1}, 1360 cm^{-1}, 1509 cm^{-1}, 1572 cm^{-1}, and 1647 cm^{-1}. These peaks correspond to the known vibrational modes of Rh6G. Although the intensity of these peaks is reduced and the signal-to-noise ratio is higher than that of the powdered reference, their enhanced visibility can be attributed to the Surface-Enhanced Raman Scattering (SERS) effect. The spectral features closely aligned with those of pure Rh6G, confirming the substrate's ability to amplify signals that are often undetectable using conventional methods.

Notably, even at ultralow concentrations (down to 10^{-9} M), the characteristic Raman peaks of rhodamine 6G remained detectable. As shown in Figure 8, the Raman spectrum of the Rh6G-analyte at a concentration of 10^{-9} M, deposited on the AuNP substrate and excited with a 532 nm laser, maintained distinct spectral signatures that closely resembled those of the reference Rh6G spectrum. This outcome attests to the reliability of the system for ultra-trace-level detection. Although some peak intensities diminished and minor spectral shifts or overlaps occurred compared to those of powdered Rh6G, the core vibrational features persisted. These findings exemplify the efficacy of the AuNP-based SERS system in enhancing signal detection at nanomolar concentrations.

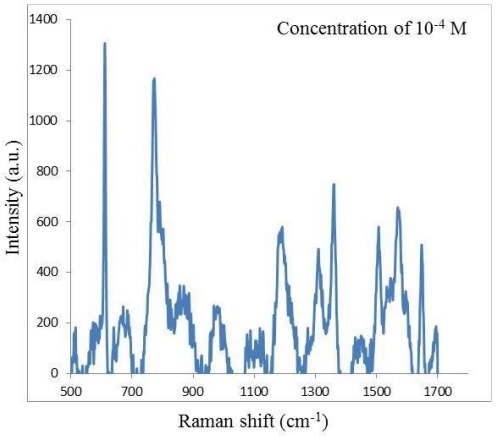

Figure 7. Raman spectrum of Rh6G at concentration of 10^{-4} M on AuNPs/SERS.

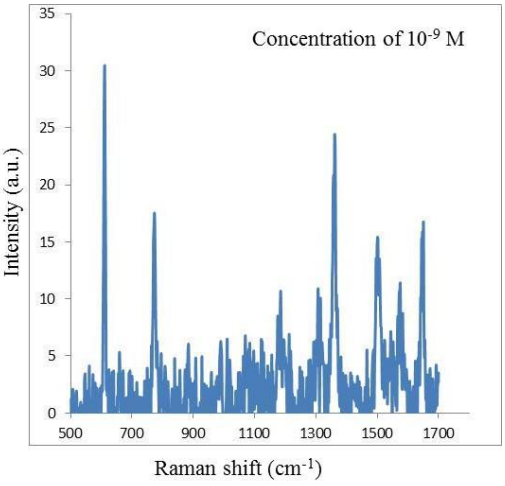

Figure 8. Raman spectrum of Rh6G at 10^{-9} M concentration on AuNPs/SERS.

This remarkable sensitivity arises from the synergistic action of two fundamental enhancement mechanisms in SERS: electromagnetic (EM) and chemical (CM) enhancement. EM enhancement originates primarily from localized surface plasmon resonance (LSPR), which creates intense electromagnetic fields at nanogaps or nanoscale "hot spots" between closely spaced particles on the AuNP surface. In contrast, CM enhancement is influenced by several factors, including the molecular structure of Rh6G, its orientation when adsorbed onto AuNPs, and the excitation wavelength employed. Substantial experimental and theoretical evidence supports the contributions of both mechanisms to overall signal amplification.

To understand how these mechanisms operate, consider the key example of surface plasmon resonance (SPR). When the laser frequency aligns with the natural oscillation frequency of the conduction electrons in the AuNPs, a strong localized surface plasmon resonance generates a highly amplified electric field near the nanoparticle surface. This enhanced field dramatically boosts the Raman signal of adjacent molecules, including adsorbed Rh6G. The dynamic interaction between these SPR-driven electromagnetic effects and the chemical properties of the analyte underpins the exceptional detection power of the system, which approaches single-molecule sensitivity under optimal conditions.

Building on this understanding, the preserved vibrational features observed in low-concentration spectra provide compelling evidence of how effectively the plasmonic effect of the AuNP substrate compensates for minimal analyte quantities. Although minor spectral variations, such as intensity fluctuations or slight peak shifts, may arise from differences in adsorption geometry or local field inhomogeneities across the substrate, the predominant enhancement mechanism ensures reliable and reproducible signal detection. This robustness makes SERS a practical analytical tool even when working with trace amounts of target molecules.

4. Conclusions

Accurate characterization of chemical residues is essential for maintaining the safety and hygiene of municipal drinking water. In this study, a standard Raman spectrometer was combined with a surface-enhanced Raman scattering (SERS) substrate based on gold nanoparticles (AuNPs) to achieve high sensitivity in detecting Rhodamine 6G (Rh6G), a surrogate for chemical residues, at concentrations ranging from 10^{-4} M to 10^{-9} M. A SERS layer with a thickness of approximately 30 - 54 nm was fabricated by depositing synthesized gold nanoparticles, 10- 20 nm in diameter, onto an NH_2-modified glass substrate. The characteristic Raman peaks of Rh6G were clearly detected on the AuNP layer at concentrations as low as 10^{-9} M, whereas no signals were observed on the glass surface even at concentrations up to 10^{-4} M. This difference demonstrates the significant Raman signal enhancement provided by the SERS-based AuNP layer, which is applicable for the detection of various chemical residues in tap water. This approach enables precise detection of trace contaminants using a handheld Raman spectrometer, representing a substantial advancement in public health protection.

Acknowledgements

The author thanks Assoc. Prof. Nghiem T. Ha Lien, a researcher of IOP, VAST, and Ms. Nguyen T. Mo, a senior undergraduate student, Fac. of Engineering Physics & Nanotechnology, University of Engineering and Technology, VNU, for experimental work on

gold nanoparticle (AuNP) synthesis and SERS based on AuNP preparation.

References

[1] S. D. Richardson, T. A. Ternes, Water Analysis: Emerging Contaminants and Current Issues, *Analytical Chemistry*, Vol. 94, 2022, pp. 382-416, https://doi.org/10.1021/acs.analchem.1c04640.

[2] P. Kovalakova, L. Cizmas, T. J. McDonald, V. K. Sharma, Occurrence and Toxicity of Antibiotics in the Aquatic Environment: A Review, Chemosphere, Vol. 251, 2020, pp. 126351, https://doi.org/10.1016/j.chemosphere.2020.126351.

[3] A. Krzyszczak, B. Czech, Occurrence and Toxicity of Polycyclic Aromatic Hydrocarbons Derivatives in Environmental Matrices, Science of the Total Environment, Vol. 788, 2021, pp. 147738, https://doi.org/10.1016/j.scitotenv.2021.147738.

[4] S. A. Snyder, P. Westerhoff, Y. Yoon, D. L. Sedlak, Pharmaceuticals, Personal Care Products, and Endocrine Disruptors in Water: Implications for the Water Industry, *Environmental Engineering Science*, Vol. 20, 2004, pp. 449-469, https://doi.org/10.1089/109287503768335931.

[5] R. P. Schwarzenbach, B. I. Escher, K. Fenner, T. B. Hofstetter, C. A. Johnson, von U. Gunten, B. Wehrli, The Challenge of Micropollutants in Aquatic Systems, *Science*, Vol. 313, 2006, pp. 1072- 077, https:// doi.org/10.1126/science.1127291.

[6] L. Molnarova, T. Halesova, M. Vaclavikova, Z. Bosakova, Monitoring Pharmaceuticals and Personal Care Products in Drinking Water Samples by the LC-MS/MS Method to Estimate Their Potential Health Risk, Molecules, Vol. 28, 2023, pp. 5899, https://doi.org/10.3390/molecules28155899.

[7] S. Schlücker, Surface-Enhanced Raman Spectroscopy: Concepts and Chemical Applications, Angew Chem Int Ed Engl, Vol. 5, 2014, pp. 4756-4795, https://doi.org/10.1002/anie. 201205748.

[8] B. Sharma, R. Frontiera, A. I. Henry, E. Ringe, SERS: Materials, Applications, and the Future. Materials Today, Vol. 15, No. 1-2, 2012, pp. 16-25, https://doi.org/10.1016/S1369-7021(12)70017-2.

[9] L. Wang, S. Pang, G. Zhou, Recent Advances in Spectroscopy Technology for Trace Analysis of Persistent Organic Pollutants, Applied Sciences, Vol. 9, 2019, pp. 3439, https://doi.org/10.3390/app91734399173439.

[10] L. Wang, Z. Wang, LiLi, J. Zhang et. al., Magnetic-Plasmonic Ni@Au Core-Shell Nanoparticle Arrays and their SERS Properties, RSC Advances, Vol. 10, 2020, pp. 2661-2669, https://doi.org/ 10.1039/c9ra10354f.

[11] K. S. Wang, H. T. Lin, W. J. Wen, L. Y. Huang, Thiol-functionalized Mesoporous Silica-Embedded AuNPs with Highly Sensitive Substrates for Surface-Enhanced Raman Scattering Detection, Surface and Coatings Technology, Vol. 483, 2024, pp. 130814, https://doi.org/10.1016/j.surfcoat.2024.130814.

[12] C. Y. Chiang, T. Y Liuang, R. J. Jeng, Au Nanoparticles Immobilized on Honeycomb-Like Polymeric Films for Surface-Enhanced Raman Scattering (SERS) Detection, Polymers, Vol. 9, 2017, pp. 93-110, https://doi.org/10.3390/polym 9030093.

[13] W. Fang, X. Zhang, Y. Chen, L. Wan et. al., Portable SERS-enabled Micropipettes for Microarea Sampling and Reliably Quantitative Detection of Surface Organic Residues, *Analytical Chemistry*, Vol. 87, 2015, pp. 9217-9224, https://doi.org/10.1021/acs.analchem.5b01635.

[14] J. Dong, P. L. Carpinone, G. Pyrgiotakis, P. Demokritou, B. M. Moudgil, Synthesis of Precision Gold Nanoparticles Using Turkevich Method, KONA Powder and Particle Journal, Vol. 37, 2020, pp. 224-232, https://doi.org/10.14356/kona.2020011.

[15] A. F. Oliveira, A. C. Pereira, M. A. C. Resende, L. F. Ferreira, Gold Nanoparticles: A Didactic Step-by-Step of the Synthesis Using the Turkevich Method, Mechanisms, and Characterizations, Analytica, Vol. 4, 2023, pp. 250-263, https://doi.org/10.3390/analytica4020020.